Superfluid density in quasi-one-dimensional systems

A. Kotani, K. Yamashita, and D. S. Hirashima
Department of Physics, Nagoya University, Nagoya 464-8602, Japan
(Received 4 January 2011; revised manuscript received 18 April 2011; published 23 May 2011)

The helicity modulus in a quasi-one-dimensional classical *XY* model is calculated with the Monte Carlo method in connection with recent experiments on liquid He in quasi-one-dimension. The helicity modulus, which is closely related to superfluid density, is strongly reduced by phase slippage. However, the effect of phase slippage is not necessarily probed in a dynamical experiment. Two methods to calculate the helicity modulus that are not affected by phase slippage are proposed: One is to use a boundary condition that prohibits phase slippage and the other is to restrict the Monte Carlo sampling to samples without phase slippage. It is then found that the helicity modulus can survive at such a high temperature as the Kosterlitz-Thouless transition temperature (in films) or the bulk transition temperature (in bars) even in the one-dimensional limit. A remarkable difference in the number of thermal vortex excitations between the cases with a film and a bar is then pointed out. The relevance of the present results to recent experiments on the superfluidity of quasi-one-dimensional He is discussed.

DOI: 10.1103/PhysRevB.83.174515 PACS number(s): 67.25.dj, 67.25.bh, 64.60.De

I. INTRODUCTION

Wada and coworkers succeeded in introducing He atoms into one-dimensional pores of a porous material, FSM (folded sheet mesoporous material) 16.[1–4] FSM-16 has a regular array of one-dimensional channels whose diameter R is systematically controlled from $R = 15$ Å to 47 Å. Typical length of pores is 2000–3000 Å. In their experiments,[3,4] ^{4}He atoms are adsorbed not only on the outer surface of the substrate but also on the inner walls of pores. They then measured superfluid density using a torsional oscillator. Separating the contribution of the one-dimensional part from that of the outer surface, they found that the onset temperature of the superfluidity in the one-dimensional part is as high as the Kosterlitz-Thouless (KT) transition temperature,[5–8] which is determined by the areal density of He atoms.

Taniguchi and Suzuki also studied superfluidity of ^{4}He confined in pores of FSM-16.[9–11] In contrast to Wada and coworkers' experiments,[3,4] they immersed the sample into bulk ^{4}He, and pores were filled with liquid ^{4}He. They also measured superfluid density with a torsional oscillator. They found not only an abrupt increase in the resonance frequency corresponding to the superfluid transition of the bulk liquid, but also a second increase in the frequency at a lower temperature. They ascribed it to the onset of superfluidity in the one-dimensional pores.[9–11]

Thus, results are quite different between the two similar experiments. Under the full-pore condition,[9–11] the onset behavior characteristic of a one-dimensional system is observed. In films, no clear evidence for the superfluid onset characteristic of one dimension is found,[3,4] although it was reported that a second increase in the resonance frequency is observed at a particular value of pore diameter, 24 Å.[12] In this paper, we discuss a possible reason for the difference between the two experiments. We should note that three-dimensionality plays little role in these experiments, in contrast to previous experiments using interconnected porous materials.[13–18]

Superfluidity in one dimension or quasi-one-dimension has long been discussed by many authors.[19–22] Shevchenko argued[19] that the characteristic temperature for one-dimensional superfluidity is given by

$$T_c \sim \frac{\hbar^2 n_1}{k_B M \ell_z}, \tag{1}$$

where n_1 is the one-dimensional number density of boson atoms, M the atomic mass, and ℓ_z the one-dimensional length of the system. It vanishes as $\ell_z \to \infty$ with n_1 being fixed. At the same time, he argued[19] that superfluid behavior could be observed at much higher temperature than T_c when $\omega\tau \gg 1$, where ω is the frequency at which superfluidity is observed (e.g., the frequency of a torsional oscillator) and τ is the relaxation time of the superflow. A similar argument was given by Machta and Guyer.[22] They pointed out that there can be two definitions of superfluid density. One is denoted by ρ_s in this study, which is the coefficient of the increase in the free energy in the presence of infinitesimal phase gradient, and the other by ρ_p,[23] which is the coefficient of the increase in the free energy in the presence of infinitesimal phase twist between both ends of the system, that is, the increase in the free energy under a twisted boundary condition. They derived[22] the relation

$$\rho_p(T) \simeq 2L_{\rm eff}\frac{k_B T}{\overline{J}} \exp\left[-\frac{L_{\rm eff}}{2\rho_s(T)}\frac{k_B T}{\overline{J}}\right] \tag{2}$$

at $T \gg \rho_s J/(k_B L_{\rm eff})$, where $L_{\rm eff} = \ell_z/(n_1 a^2)$, $\overline{J} = \hbar^2/(Ma^2)$, and a^D is the area ($D = 2$) or volume ($D = 3$) per atom. [They derived the expression for $D = 2$ (for ^{4}He films on a cylindrical surface). The extension to the case with $D = 3$ (for ^{4}He filling pores) is straightforward.] In both cases, $L_{\rm eff}$ is the effective length of the system. Here the superfluid densities are normalized so that $\rho_{s,p}(T = 0) = 1$. ρ_p suffers from phase slippage and vanishes at $T \gtrsim \overline{J}\rho_s/(k_B L_{\rm eff}) \simeq \hbar^2 n_1/(k_B M \ell_z) \sim T_c$. This is because the energy of a state with finite superflow vanishes in proportion to $1/\ell_z$ in the limit of $\ell_z \to \infty$. In contrast to ρ_p, $\rho_s(T)$ is not affected by phase slippage and can remain finite at higher temperatures. They further argued that it is ρ_s that is observed in torsional oscillator experiments,[22]

because the motion of the substrate establishes an external superfluid velocity over the entire area of the film rather than a phase twist from one side of the film to the other.[24] Another relation between the two superfluid densities was also derived by Prokof'ev and Svistunov.[25] They pointed out that the difference between the two definitions can be relevant in (quasi-)one dimension.[25,26]

The experimental results mentioned above can then be partly understood by these theories. If the condition $\omega\tau \gg 1$ holds in Wada and coworkers' experiments,[3,4] it may be natural that superfluidity is observed at such a high temperature as the KT transition temperature. On the other hand, in the full-pore experiments by Taniguchi and Suzuki,[9–11] the opposite condition, $\omega\tau \ll 1$, seems to hold so that ρ_p is observed and the onset is at a temperature characteristic of one-dimensional superfluidity.

However, a few questions remain unanswered. One of them is what the explicit temperature dependence of $\rho_s(T)$ is. If $L_{\rm eff}$ is sufficiently large, $\rho_p(T)$ vanishes at an extremely low temperature. Then, $\rho_s(T)$ in Eq. (2) can be approximated by $\rho_s(T=0)$. In this case, the explicit temperature dependence of $\rho_p(T)$ is obtained without knowledge of that of $\rho_s(T)$. In full-pore experiments using nanopores of diameter $R \sim 40$ Å, $L_{\rm eff} \simeq 8$. In such a case, the temperature dependence of $\rho_s(T)$ may matter. The earlier theoretical investigations[19,22,25] did not give an explicit temperature dependence of $\rho_s(T)$. Naively, one may expect that the temperature dependence of $\rho_s(T)$ is the same as that in the bulk. However, it may be too naive to expect that it holds for any ℓ_z (or $L_{\rm eff}$).

Recently, the superfluid density in one dimension has also been studied within the Tomonaga-Luttinger liquid (TLL) theory.[27,28] The expression for superfluid density obtained in these studies is similar to the one by Machta and Guyer,[22] and no explicit temperature dependence of $\rho_s(T)$ is given, either. Explicit temperature dependence of superfluid density in (quasi-)one dimension has recently been investigated using a classical XY model[29] and an interacting boson model.[30,31] The results are consistent with the prediction of the earlier studies. Again, we emphasize that the focus of these investigations was on $\rho_p(T)$ and the temperature dependence of $\rho_s(T)$ was not explicitly calculated. Therefore, it is desirable to be able to calculate $\rho_s(T)$, in addition to $\rho_p(T)$, using a microscopic model. This is one of the purposes of this work.

Another issue that must be addressed is the difference between the two experiments: One is on ^{4}He films adsorbed on nanopores[3,4] and the other is on ^{4}He filling nanopores.[9–11] One could say that the difference is because of the difference in the value of $\omega\tau$; however, it is still unclear why it can be so different. To understand the possible reason behind this difference is another purpose of this work.

In this study, we use a classical XY model to study superfluid density in quasi-one-dimension. A hard-core boson system can be mapped to a quantum XY model.[32] Many microscopic details, such as the precise form of the adsorption potential of the substrate, the degree of randomness of the surface, and so on, in the experiments are unknown at present. In this study, discarding these details, we use the simplest possible model to consider superfluidity in nanopores. Then, in addition to the classical approximations, we consider only the exchange interaction between xy components of spins on the nearest-neighbor sites neglecting the effect of interatomic interaction working at finite distances. Moreover, the exchange interaction is assumed to be independent of the position (except in Sec. V); the effect of adsorption potential is not considered. Due to these simplifications, the results obtained in this study would be only of qualitative relevance to ^{4}He systems in reality and quantitative comparison is difficult. However, qualitative results obtained in this study can be useful for understanding the experiments on quasi-one-dimensional ^{4}He. Recently, cold atoms confined in a quasi-one-dimensional trap have been successfully prepared and their physical properties are extensively studied.[33–36] Possible superfluid behavior is of much interest. This study may also be useful for studies of those systems.

In the next section, we introduce the model, summarize the results obtained so far, and introduce quantities of interest in this study. In Sec. III, we propose a method to calculate $\rho_s(T)$ and show the numerical results of $\rho_s(T)$ in films and bars. Then, in Sec. IV, we introduce another method to calculate $\rho_s(T)$. In doing so, we clarify an important difference between the case with films and with bars. In Sec. V, we study the effect of possible randomness on the surface of nanopores. The final section is devoted to a summary and discussion.

II. QUASI-ONE-DIMENSIONAL XY MODEL: HELICITY MODULUS, PHASE WINDING, AND VORTEX-PAIR DENSITY

A hard-core boson system can be mapped to a ferromagnetic XY model by introducing a fictitious lattice into the system.[32] In the mapping, we have to specify the lattice constant d. It is natural to assume that d is comparable with (or slightly larger than) the average particle-particle distance a, that is, $d \simeq a$. Exchange interaction J can then be estimated as $J \simeq \hbar^2/(2md^2)$,[32] where m is the mass of a ^{4}He atom. Considering $d \simeq a$, the exchange interaction J can be written as $J \simeq \hbar^2 n_1/(2m\ell_x)$ in ^{4}He films adsorbed on inner surfaces of nanopores, where ℓ_x is the width of films (the circumference of nanopores). In liquid ^{4}He filling nanopores, $J \simeq \hbar^2 n_1 d/(2ms)$, where s is the cross-sectional area of nanopores.

To study ^{4}He films adsorbed on nanopores, we consider an XY model on a square lattice measuring $L_x \times L_z$, where $L_\mu = \ell_\mu/d$ $(\mu = x,z)$ with $L_x \ll L_z$ (a film). We impose the periodic boundary condition in both (x and z) directions. For ^{4}He filling nanopores, we consider an XY model on a cubic lattice measuring $L_x \times L_y \times L_z$ with $L_x = L_y$ and $L_x \ll L_z$ (a bar). In this case, $L_x = L_y \simeq \sqrt{s}/d$. We impose the periodic boundary condition in the z direction and open boundary condition in the other directions. Note that the effective length $L_{\rm eff}$ is $L_{\rm eff} = L_z/L_x = \ell_z/\ell_x$ in films, and $L_{\rm eff} = L_z/L_xL_y \simeq \ell_z d/s$ in bars. In a film, $L_{\rm eff}$ is its aspect ratio and is independent of d. In a bar, it depends on the lattice constant d and is not determined only by the geometry of the system.

In this work, we consider classical XY models. Certainly, quantum effects are important in low dimensions; a one-dimensional quantum XY model has no long-range order even at $T = 0$ while the classical counterpart does. However, a classical model turns out to be useful in discussing qualitative

superfluid property. The temperature dependence of superfluid density in one dimension calculated with a classical *XY* model[29] is similar to that calculated for an interacting boson model and also to the prediction of the TLL theory,[30] if the coupling constant is appropriately replaced, except at extremely low temperatures.

Thus, we consider the *XY* model defined as

$$\mathcal{H} = -J \sum_{\langle \boldsymbol{n},\boldsymbol{n}' \rangle} \cos[\theta(\boldsymbol{n}) - \theta(\boldsymbol{n}')], \tag{3}$$

where $\theta(\boldsymbol{n})$ stands for the direction of the spin vector at lattice point $\boldsymbol{n}$ and J represents the exchange interaction between the nearest-neighbor pairs $\langle \boldsymbol{n},\boldsymbol{n}' \rangle$. The total number of lattice points is $N = L_x L_z$ for a square lattice (a film) and $N = L_x L_y L_z = L_x^2 L_z$ for a cubic lattice (a bar).

We calculate various quantities with the Monte Carlo method. In doing so, we use Wolff's algorithm.[37] We typically collect $(1\text{–}5) \times 10^6$ samples after discarding $(1\text{–}5) \times 10^4$ thermalization steps.

We calculate the helicity modulus Υ along the z axis. Superfluid density is a tensor, and it is the z component that is relevant in the experiments. Υ is defined as the coefficient of the increase in the free energy under a twisted boundary condition in the z direction and is given by[38]

$$\Upsilon = \frac{1}{N} \left\langle \sum_{\boldsymbol{n}} \cos[\theta(\boldsymbol{n} + \hat{z}) - \theta(\boldsymbol{n})] \right\rangle - \frac{J}{N k_B T} \left\langle \left\{ \sum_{\boldsymbol{n}} \sin[\theta(\boldsymbol{n} + \hat{z}) - \theta(\boldsymbol{n})] \right\}^2 \right\rangle. \tag{4}$$

Conventionally, it is considered[39] to be proportional to superfluid density,

$$\Upsilon \propto \rho_p. \tag{5}$$

Here, we use subscript p to distinguish it from ρ_s, which is the coefficient of the increase in the free energy in the presence of infinitesimal phase gradient. Even if the phase twist between both ends of the system is infinitesimally small, the phase gradient is not necessarily so and superflow of finite velocity can flow between both ends, because the phase twist has uncertainty of $2\pi I$, where I is an integer. If the energy of a state with nonzero I is much higher than the ground-state energy, it makes little contribution to superfluid density. However, in quasi-one-dimension, the energy decreases as $2\pi^2 J I^2 / L_{\rm eff}$ in the limit of $L_{\rm eff} \to \infty$ and then phase slippage can contribute to the decay of superflow even at low temperatures.

Now, we define the phase winding. First, we define the phase winding in each row. For a film,

$$I(n_x) = \frac{1}{2\pi} \sum_{n_z=1}^{L_z} [\theta(n_x,n_z+1) - \theta(n_x,n_z)], \tag{6}$$

where $[\cdots]$ is defined so that $|[\cdots]| \leqslant \pi$. $I(n_x)$ is an integer because of the periodic boundary condition in the z direction. Then, we define $I_{\rm tot}$ (and $i_{\rm tot}$) as

$$i_{\rm tot} = \frac{1}{L_x} I_{\rm tot} = \frac{1}{L_x} \sum_{n_x=1}^{L_x} I(n_x). \tag{7}$$

The thermal average of $I_{\rm tot}$ must vanish, because the probability of a state with $I_{\rm tot}$ is equal to that with $-I_{\rm tot}$. We then define a quantity representing the degree of phase winding, i_W^2,

$$i_W^2 = \frac{1}{L_x} \sum_{n_x=1}^{L_x} \langle I(n_x)^2 \rangle. \tag{8}$$

For a bar, we can define similar quantities. For example,

$$I(n_x,n_y) = \frac{1}{2\pi} \sum_{n_z=1}^{L_z} [\theta(n_x,n_y,n_z+1) - \theta(n_x,n_y,n_z)] \tag{9}$$

and

$$i_{\rm tot} = \frac{1}{L_x L_y} I_{\rm tot} = \frac{1}{L_x L_y} \sum_{n_x=1}^{L_x} \sum_{n_y=1}^{L_y} I(n_x,n_y). \tag{10}$$

In films, vortices always appear as a vortex-antivortex pair under the periodic conditions in both directions. Vorticity can be defined as[40]

$$\begin{aligned} v(\boldsymbol{n}) = \frac{1}{2\pi} \{ & [\theta(n_x+1,n_y) - \theta(n_x,n_y)] \\ & + [\theta(n_x+1,n_y+1) - \theta(n_x+1,n_y)] \\ & + [\theta(n_x,n_y+1) - \theta(n_x+1,n_y+1)] \\ & + [\theta(n_x,n_y) - \theta(n_x,n_y+1)] \}. \end{aligned} \tag{11}$$

Essentially, $v(\boldsymbol{n}) = 0$ and ± 1,[40] and $\sum_{\boldsymbol{n}} \langle v(\boldsymbol{n}) \rangle = 0$. We define vortex-pair density ρ_v as

$$\rho_v = \frac{1}{2 L_x L_z} \sum_{\boldsymbol{n}} \langle |v(\boldsymbol{n})| \rangle \tag{12}$$

in films.

Note that while $I_{\rm tot}$ takes only integer values, $i_{\rm tot}$ is not necessarily an integer. Let us first assume that $I(n_x) = 0$ for all n_x's; that is, there is neither phase slippage nor vortices. When only phase slippage occurs, $i_{\rm tot}$ takes an integer value. On the other hand, if a vortex is created at (n_1,n_y) and an antivortex at (n_2,n_y') $(n_1 > n_2)$, then $I(n_x) = 1$ (0) at $n_2 + 1 \leqslant n_x \leqslant n_1$ and $I(n_x) = 0$ (-1) otherwise. Then, $i_{\rm tot}$ can assume a noninteger value.

In bars, there are two kinds of vortices: vortices whose ends are on the surface of a bar and vortex rings. Looking only at the surface, the ends of one vortex can be regarded as a vortex and an antivortex. Discarding vortex rings,[41] the quantity defined by Eq. (12), where the summation is over the lattice points on the surface of a bar and the normalization $1/(2L_xL_y)$ should be replaced by $1/[4(L_x + L_y - 2)L_z]$, represents the number of vortices (per surface area) in the system.

Figure 1(a) shows the temperature dependence of Υ on a square lattice whose size is $N = 16 \times 480$ and $L_{\rm eff} = L_z/L_x = 30$. It can be seen that Υ rapidly decreases from unity as T increases. The temperature dependence can be expressed by $\Upsilon = C \exp[-L_{\rm eff} k_B T/(2J)]$ where C depends on $L_{\rm eff} k_B T/J$ (and $k_B T/J$) for $k_B T \gg J/L_{\rm eff}$.[29,43] This expression is consistent with that obtained by Machta and Guyer.[22] The linear temperature dependence at low temperatures is a consequence of the classical approximation; $\Upsilon \simeq 1 - k_B T/(2DJ)$ when $L_x, L_z \to \infty$ ($D = 2$ for films, and $D = 3$ for bars). From Fig. 1(b), we can see that vortex

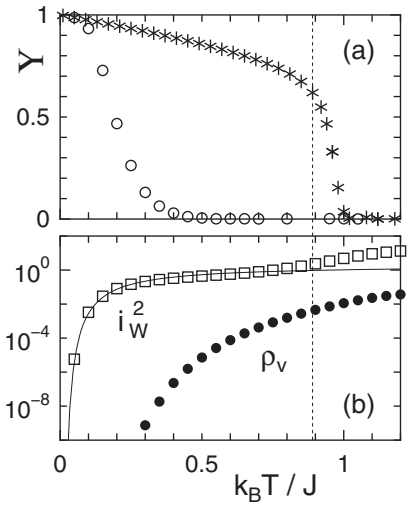

FIG. 1. (a) Helicity modulus Υ in the z direction in the 2D XY model on a lattice $N = 16 \times 480$. For comparison, Υ for $N = 160 \times 160$ is also shown (stars). (b) Vortex-pair density ρ_v (closed dots) and phase winding i_W^2 (open squares) in the 2D XY model ($N = 16 \times 480$). Thin solid curve stands for the result with the spin-wave approximation ($i_W^2 \simeq 2\exp[-2\pi^2 J/(L_{\rm eff}k_BT)]$).[29] Error bars are smaller than the size of symbols. The vertical dotted line stands for the KT transition temperature $T_{\rm KT} = 0.89J/k_B$.[42]

pairs hardly contribute to the reduction of Υ, and it is phase slippage, that is, finite i_W^2, that causes Υ to vanish. The same is true in a bar of size $N = 4 \times 4 \times 480$ as can be seen from Fig. 2; the effective length $L_{\rm eff}$ is also $L_{\rm eff} = L_z/L_x^2 = 30$ here. We note that the temperature dependence of i_W^2 (and therefore

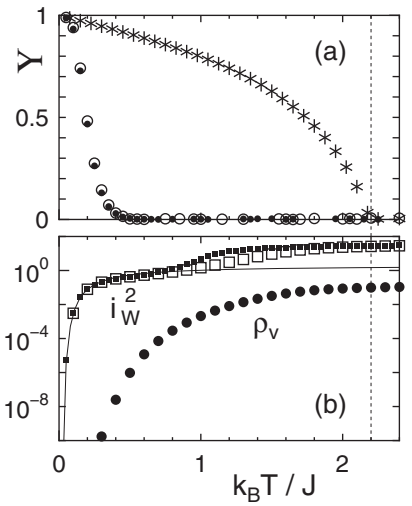

FIG. 2. (a) Helicity modulus Υ in the z direction in the 3D XY model on a lattice $N = 4 \times 4 \times 480$ (open dots). For comparison, Υ for $N = 40 \times 40 \times 40$ is also shown (stars). Small closed dots represent Υ in the 2D XY model ($N = 16 \times 480$). (b) Vortex density ρ_v (closed dots) and phase winding i_W^2 (open squares) in the 3D XY model ($4 \times 4 \times 480$). Thin solid curve stands for the result with the spin-wave approximation ($i_W^2 \simeq 2\exp[-2\pi^2 J/(L_{\rm eff}k_BT)]$).[29] Small closed squares represent ρ_v in the 2D XY model ($N = 16 \times 480$). Error bars are smaller than the size of symbols. The vertical dotted line stands for the bulk transition temperature $T_\lambda = 2.20J/k_B$.[44]

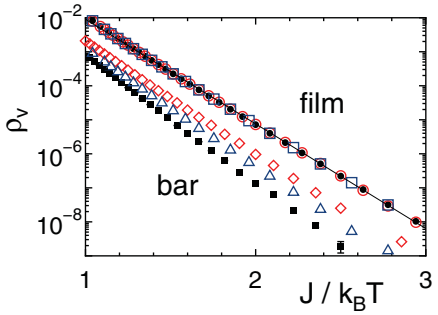

FIG. 3. (Color online) Vortex(-pair) density ρ_v as a function of inverse temperature for different system sizes: $N = 16 \times 480$ (open dots), 32×480 (open squares), 160×160 (closed dots), $4 \times 4 \times 480$ (open diamonds), $8 \times 8 \times 480$ (triangles), and $40 \times 40 \times 40$ (closed squares). Solid line is the result of fitting.

of Υ) in a film is the same as that in a bar at low temperatures for the same value of $L_{\rm eff}$.[29]

From the behavior of $\rho_v(T)$ at low temperatures, we can measure the energy necessary for creation of a vortex pair in 2D (a vortex in 3D). The vortex density $\rho_v(T)$ depends on temperature exponentially at low temperatures, $\rho_v(T) \sim \exp[-E_v/(k_BT)]$. Figure 3 shows the logarithmic plot of $\rho_v(T)$ as a function of $1/T$. In films, ρ_v hardly depends on the size. Usually, the energy required for creation of a vortex pair is denoted by 2μ. We can estimate $E_v/J = 2\mu/J = 7.19 \pm 0.01$ for a lattice $N = 160 \times 160$ and results for different system sizes agree within errors. This is smaller than the earlier results.[40,45,46] Here, we used the data between 10^{-6} and 10^{-4}, $10^{-6} < \rho_v(T) < 10^{-4}$, in the estimation of E_v; this corresponds to the temperature range $0.44J \lesssim k_BT \lesssim 0.62J$ in films.[47] (The quality of data at lower temperatures gradually deteriorates.) If we also used the data at higher temperatures, we would obtain a larger value of 2μ, consistently with the earlier results. In contrast to the case with films, $\rho_v(T)$ slightly depends on the size in bars. This is because there are "corners" in the bars studied here. For $N = 4 \times 4 \times 480$, we find $E_v/J = 7.75 \pm 0.01$, for $N = 8 \times 8 \times 480$, $E_v/J = 8.20 \pm 0.02$, and for $N = 40 \times 40 \times 40$, $E_v/J = 8.96 \pm 0.01$. In Appendix A, we discuss the case with bars without corners.

III. SUPERFLUID DENSITY WITHOUT CONTRIBUTIONS OF PHASE SLIPPAGE. I

Whether the superfluid density ρ_p can be observed or not depends on the value of $\omega\tau$. τ is the time necessary for phase slippage to occur and must depend on temperature as $\tau \propto \exp[\Delta F/(k_BT)]$, where ΔF is the free-energy barrier that the system has to get over in the process of phase slippage.[48] If $\omega\tau \gg 1$, no phase slippage occurs during one period of a torsional oscillator. In this case, ρ_p is not observed and it is ρ_s that is observed. In this section we propose a method to calculate $\rho_s(T)$, which is not affected by phase slippage.

Both 2D films and 3D bars can be viewed as tori under the periodic boundary condition. A vortex pair in a film or a vortex in a bar is generated when a vortex filament pierces the surface of a torus. Suppose that the system is in a state of $i_{\rm tot} = 0$ in the beginning and that a vortex filament comes from the outer space, pierces the surface [creates a vortex(-pair)], drifts

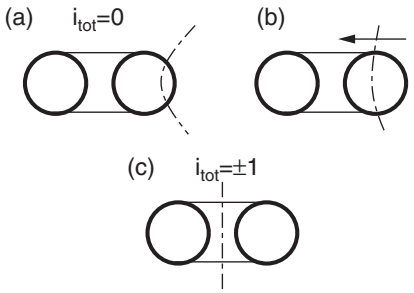

FIG. 4. Cross-sectional view of a torus. (a) A vortex filament pierces the surface of a torus, creating a vortex-pair in a film or a vortex in a bar. (b) Inward drift of a vortex filament. (c) A vortex filament passes through to the center of a torus, annihilating a vortex pair (or a vortex) and leaving the state with $i_{\rm tot} = \pm 1$ (depending on the direction of the filament).

inward, and passes through to the center of a torus. Then, a created vortex(-pair) is annihilated and the system is shifted to a state with $i_{\rm tot} = 1$ or -1. See Fig. 4. This is the elementary process of phase slippage, and ΔF (at $T = 0$) corresponds to the energy of the state where a vortex and an antivortex are maximally separated. It must be larger than E_v estimated in the previous section, because attractive interaction acts between a vortex and an antivortex.

One of the simplest ways to prevent phase slippage is to close the hole in the center of a torus. This can be done by imposing a specific boundary condition, that is, by replacing all the spins in a row in a film by a single spin,

$$\theta(n_0,n_z) = \theta(n_0), \tag{13}$$

for a specific value of $n_x = n_0$. We call this boundary condition the no-phase-slippage boundary condition (NPSBC) in this study. Under the NPSBC, while translational symmetry in the x direction is broken, translational symmetry in the z direction and rotational symmetry in spin space are conserved. $\theta(n_0)$ interacts with $2L_z$ spin variables, $\theta(n_0 \pm 1,n_z)$, and rotates accordingly. Under the NPSBC, a state with $I(n_x) \neq 0$ is necessarily accompanied by vortex pairs. For a bar, we can similarly consider the NPSBC. We replace spins on all the lattice points on a corner of the bar, say $n_x = n_y = 1$, by a single spin.[49] Under the NPSBC, there occurs no phase slippage, and the calculated Υ can be identified with ρ_s.

Figure 5 shows the helicity modulus Υ, vortex density ρ_v, and phase winding i_W^2 in films of different sizes calculated under the NPSBC. It can be seen that phase winding i_W^2 diminishes rapidly as temperature decreases in contrast to the case with conventional periodic boundary condition (Fig. 1), and that Υ's for different system sizes almost coincide with each other for $T < T_{\rm KT}$. For $T > T_{\rm KT}$, Υ remains finite and is larger in a narrower film. This can be understood as a result of confinement of a vortex pair: When we separate a vortex and an antivortex along a pore axis, a constant restoring force works between the pair whose strength is inversely proportional to the diameter of pore.[20,21] This force strongly prevents the dissociation of a vortex pair, resulting in increase of the onset temperature of superfluidity. Originally, this conclusion was reached under the condition that the vortex core radius is much smaller than the pore circumference.[20,21] The present result implies that the conclusion holds in narrower tubes.

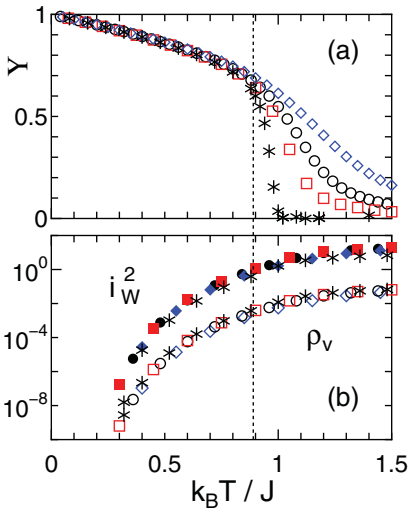

FIG. 5. (Color online) (a) Helicity modulus Υ and (b) vortex-pair density ρ_v and phase winding i_W^2 in films of different sizes calculated under the no-phase-slippage boundary condition (NPSBC): $N = 8 \times 480$ (diamonds), 16×480 (dots), and 32×480 (squares). For comparison, results for $N = 160 \times 160$ under the conventional boundary condition are also shown (stars). The dotted line represents the location of the KT transition temperature $T_{\rm KT} = 0.89 J/k_B$.[42]

Figure 6 shows Υ, ρ_v, and i_W^2 in bars of different system sizes calculated under the NPSBC. Phase winding i_W^2 is again found to diminish rapidly as $T \to 0$, and Υ remains finite even at $T = T_\lambda$. In contrast to the case with films, Υ is suppressed at $T < T_\lambda$ in a bar in comparison with its counterpart in the bulk.

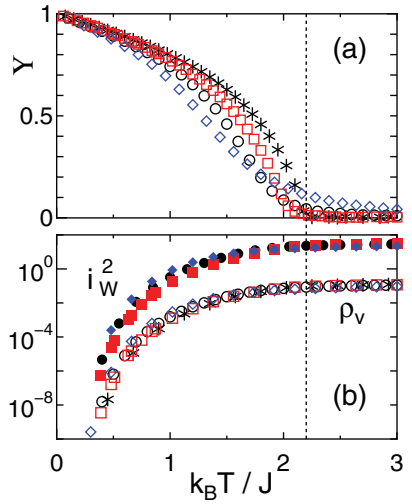

FIG. 6. (Color online) (a) Helicity modulus Υ and (b) vortex density ρ_v and phase winding i_W^2 in bars of different sizes calculated with the no-phase-slippage boundary condition (NPSBC): $N = 2 \times 2 \times 480$ (diamonds), $N = 4 \times 4 \times 480$ (dots), and $8 \times 8 \times 480$ (squares). For comparison, results for $40 \times 40 \times 40$ (stars) obtained under the conventional boundary condition are also shown (stars). The dotted line represents the bulk transition temperature $T_\lambda = 2.20 J/k_B$.[44]

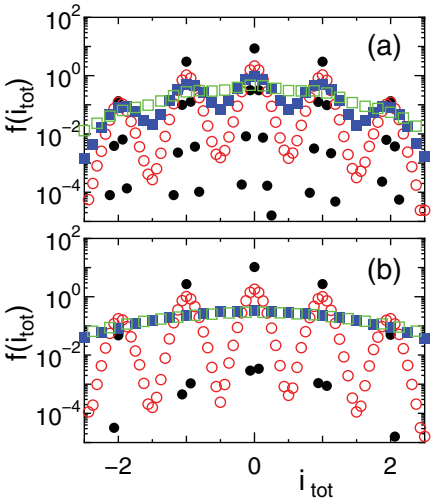

FIG. 7. (Color online) (a) Distribution function $f(i_{\rm tot})$ of phase winding $i_{\rm tot}$ for $N = 16 \times 480$ at different temperatures: $T = 0.6T_{\rm KT}$ (closed dots), $0.8T_{\rm KT}$ (open dots), $0.9T_{\rm KT}$ (closed squares), and $T_{\rm KT}$ (open squares). (b) Distribution function $f(I_{\rm tot})$ of phase winding $i_{\rm tot}$ for $N = 4 \times 4 \times 480$ at different temperatures: $T = 0.2T_\lambda$ (closed dots), $0.4T_\lambda$ (open dots), $0.6T_\lambda$ (closed squares), and T_λ (open squares).

We find that, as the system size increases, the results approach those on a lattice of size $L \times L(\times L)$ obtained under the conventional boundary condition, which has been used in Sec. II, as expected. If phase slippage is prohibited, the shape of the system does not matter and the thermodynamic limit is naturally approached when the system size is increased. In addition, the NPSBC hardly affects results on a lattice of $L \times L(\times L)$, because phase slippage does not contribute to superfluid density in these cases. Further details are discussed in Appendix B.

In both films and bars, we find that ρ_s can remain finite at such a high temperature as $T_{\rm KT}$ or T_λ even for a large $L_{\rm eff}$. However, in this method of calculation, finite size effects may be large. Consider the case with $L_x = 1$. In this case, the NPSBC makes no sense. Moreover, we have found no difference between films and bars that may suggest a possible reason for the difference in $\omega\tau$. In the next section, we propose another method for calculating $\rho_s(T)$.

IV. SUPERFLUID DENSITY WITHOUT CONTRIBUTIONS OF PHASE SLIPPAGE. II. DISTRIBUTION OF PHASE WINDING

At $T = 0$, there occurs no phase winding for a finite $L_{\rm eff}$, $I(n_x) = 0$ $[I(n_x,n_y) = 0]$ and $i_{\rm tot} = 0$. At low temperatures, no vortices are thermally excited. It is virtual vortex(-pair) excitations that create phase slippage. Then, $i_{\rm tot}$ can take finite integer values $(\pm 1, \pm 2, \cdots)$. As T further increases, vortices are thermally excited, which allows $i_{\rm tot}$ to assume noninteger values. To see this behavior, we calculate a distribution function of phase winding $i_{\rm tot}$. First, we define the number of Monte Carlo samples where $i_{\rm tot} = x$ as $F(x)$;

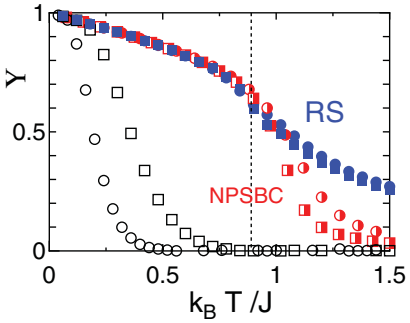

FIG. 8. (Color online) Helicity modulus Υ of 2D XY model of different sizes obtained with the restricted sampling (RS) ($|i_{\rm tot}| \leqslant 1/2$): $N = 16 \times 480$ (closed dots) and 32×480 (closed squares). For comparison, the same quantities calculated under the conventional boundary condition (open symbols; dots for $N = 16 \times 480$ and squares for $N = 32 \times 480$) and the NPSBC are also shown (half-closed symbols; dots for $N = 4 \times 320$ and squares for $N = 32 \times 480$). The dotted line represents the KT transition temperature $T_{\rm KT} = 0.89J/k_B$.[42]

$\sum_{i_{\rm tot}} F(i_{\rm tot}) = N_{\rm MC}$, where $N_{\rm MC}$ is the total number of Monte Carlo samples. Then, we define $f(i_{\rm tot})$ as

$$f(i_{\rm tot}) = \frac{L_x}{N_{\rm MC}} F(i_{\rm tot}), \tag{14}$$

for a film so that $\int dx f(x) = 1$. For a bar, L_x is replaced by $L_x L_y$.

Figure 7 shows the distribution $f(i_{\rm tot})$ in a film ($N = 16 \times 480$) and in a bar ($N = 4 \times 4 \times 480$). A prominent multipeak structure can be seen at low temperatures in both cases. The peaks at $i_{\rm tot} \neq 0$ correspond to states with finite superflow, which can be reached from $i_{\rm tot} = 0$ with phase slippage. Then, we can estimate the superfluid density that has no contributions from phase slippage by calculating helicity modulus using only the restricted Monte Carlo samples that satisfy $|i_{\rm tot}| \leqslant 1/2$. We call this method the restricted sampling (RS).

Figure 8 shows Υ calculated using the RS in films of different sizes. At $T \lesssim T_{\rm KT}$, the results agree well with those obtained using the NPSBC, implying again that ρ_s can survive at such a high temperature as $T_{\rm KT}$ even for a large $L_{\rm eff}$. However, at $T > T_{\rm KT}$, they decrease more slowly as T increases. At high temperatures, the distribution function $f(i_{\rm tot})$ does not exhibit a multipeak structure any more. In such cases, there is no longer a reason why the samples can be restricted to $|i_{\rm tot}| \leqslant 1/2$. If we insist on using the RS in calculating superfluid density, contributions from vortices are only partly considered. Therefore, at $T \gtrsim T_{\rm KT}$, Υ obtained with the RS should overestimate superfluid density ρ_s. If we increase the system size with a fixed value of $L_{\rm eff}$, we cannot obtain the bulk limit at $T \gtrsim T_{\rm KT}$. See also Appendices B and C. Figure 9 shows Υ calculated with the RS in bars. We find similar results to those in the case of films (Fig. 8). However, Υ calculated with the RS starts to deviate from its counterpart obtained using the NPSBC at a temperature below T_λ, implying that there is no longer a reason to restrict the sampling far below T_λ. Next, we further discuss this point.

Now, we return to Fig. 7. There is actually a marked difference between the results in films and bars. In films,

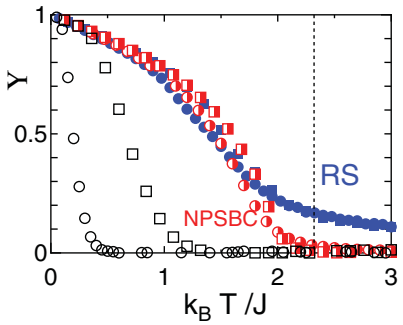

FIG. 9. (Color online) Helicity modulus Υ of 3D XY model of different sizes obtained with the restricted sampling (RS) ($|i_{\rm tot}| \leqslant 1/2$): $N = 4 \times 4 \times 480$ (closed dots) and $8 \times 8 \times 480$ (closed squares). For comparison, the same quantities calculated under the conventional boundary condition (open symbols; dots for $4 \times 4 \times 480$ and squares for $8 \times 8 \times 480$) and the NPSBC are also shown (half-closed symbols; dots for $4 \times 4 \times 480$ and squares for $8 \times 8 \times 480$). The dotted line represents the bulk transition temperature $T_\lambda = 2.20J/k_B$.[44]

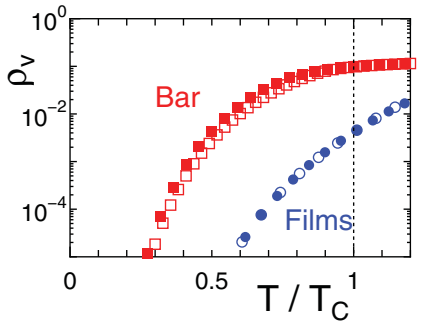

FIG. 10. (Color online) Vortex(-pair) density ρ_s in films or bars with different sizes as a function of scaled temperature T/T_c; $T_c = T_{\rm KT} = 0.89J/k_B$ in films and $T_c = T_\lambda = 2.20J/k_B$ in bars. Lattice sizes are $N = 16 \times 480$ (closed dots), 32×480 (open dots), $4 \times 4 \times 480$ (closed squares), and $8 \times 8 \times 480$ (open squares).

the multipeak structure persists at temperatures close to $T_{\rm KT}$. Even at $T = 0.9T_{\rm KT}$, we can see peaks in $f(i_{\rm tot})$. On the other hand, in bars, the peak structure is no longer observed at $T = 0.6T_\lambda$. The distribution function $f(i_{\rm tot})$ at $T = 0.6T_\lambda$ is hardly distinguishable from that at $T = T_\lambda$. For a larger value of L_x, the multipeak structure persists up to higher temperatures; however, it still vanishes at a temperature lower than T_λ.

From the depth of a valley in the distribution function, we can estimate ΔF, because the depth of a valley is considered to be $\exp[-\Delta F/(k_B T)]$. From Fig. 7, we estimate $\Delta F \simeq 4.9J$ at $T = 0.8T_{\rm KT}$ and $\Delta F \simeq 1.9J$ at $T = 0.9T_{\rm KT}$ in a film of $N = 16 \times 480$. At lower temperatures, e.g., at $0.7T_{\rm KT}$, we can only say $\Delta F \gtrsim (8$–$9)J$. For $N = 32 \times 480$, we find a larger ΔF than its value for $N = 16 \times 480$. At higher temperatures, ΔF is roughly proportional to L_x. Similarly, in a bar with $N = 4 \times 4 \times 480$, we find $\Delta F \simeq 7.6J$ at $T = 0.4T_\lambda$ and $\Delta F \simeq 0.8J$ at $T = 0.5T_\lambda$.

Thus, ΔF is found to decrease rapidly as T increases. In bars, no barrier exists at $T \simeq 0.6T_\lambda$ for $N = 4 \times 4 \times 480$. Without a free-energy barrier, $\omega\tau$ may be small enough for a large range of $i_{\rm tot}$ to be probed in the period of observation $1/\omega$. Then, $\rho_p(T)$ can be observed at temperatures far below T_λ. On the other hand, in films, the free-energy barrier persists up to temperatures close to $T_{\rm KT}$. Therefore, $\rho_p(T)$ can be observed only at temperatures close to $T_{\rm KT}$.

This difference between films and bars originates from the difference in the number of thermally excited vortices. In Fig. 10, we replot $\rho_v(T)$ as a function of temperature scaled by $T_{\rm KT}$ (in films) or T_λ (in bars). In films, we find that $\rho_v(T) \simeq 4 \times 10^{-3}$ at $T_{\rm KT} = 0.89J/k_B$.[40,45,46] In bars, ρ_v has already reached 1×10^{-3} even at $T = 0.5T_\lambda = 1.1J/k_B$. This is because the energy E_v necessary for the creation of a vortex(-pair) is not very different between the cases with films and bars.

In the presence of thermally excited vortices, additional creation of vortices or drifting away of a vortex and an antivortex is unnecessary for phase slippage (dissipation of superflow) to occur. Recombination or reconnection of existing vortices can lead to dissipation of superflow and there is no high free-energy barrier for recombination or reconnection to take place. See Fig. 11. This is why the free-energy barrier ΔF decreases so rapidly as T increases, particularly in the case of bars. For recombination to occur in films, a vortex and an antivortex have to be dissociated or, at least, only loosely bound. This also implies that recombination occurs only at temperatures close to $T_{\rm TK}$.

V. EFFECT OF RANDOMNESS ON HELICITY MODULUS

So far, we have considered uniform XY models. In real He systems, the effects of inhomogeneity caused by adsorption potential and randomness cannot be ignored. However, it is difficult to precisely know the microscopic details about these effects. In this section, we introduce bond randomness on the surface of the system and study its effect.

First, we consider a film. Instead of Eq. (1), we consider

$$\mathcal{H} = -\sum_{\langle \boldsymbol{n},\boldsymbol{n}'\rangle} J(\boldsymbol{n},\boldsymbol{n}')\cos(\theta_{\boldsymbol{n}} - \theta_{\boldsymbol{n}'}), \tag{15}$$

where $J(\boldsymbol{n},\boldsymbol{n}')$ distributes uniformly between $0 < J(\boldsymbol{n},\boldsymbol{n}') < J$. Figure 12 shows helicity modulus of this model, Eq. (15). For comparison, we also show the result of a square film ($N = 80 \times 80$). As the average strength of the exchange constant is $0.5J$, the transition temperature is reduced roughly by half. The helicity modulus at $T = 0$ is also reduced to approximately 0.4. The ratio of the onset temperature of Υ in a lattice $N = 16 \times 480$ to the reduced KT transition temperature is close to that without randomness. However, the distribution function $f(i_{\rm tot})$ is considerably different from

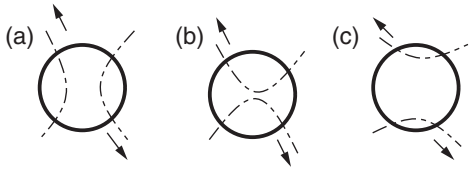

FIG. 11. Cross section of a torus. In the presence of thermally excited vortices (a), reconnection of vortices (b) can be an easy way to dissipate superflow. A vortex and an antivortex in a film need not drift against attractive interaction (c).

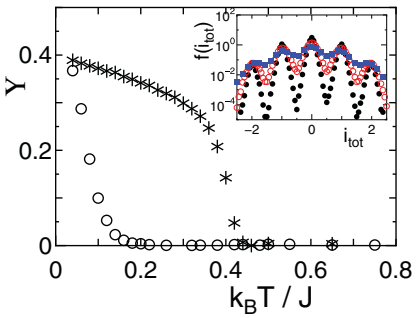

FIG. 12. (Color online) Helicity modulus Υ in the random-bond XY model, Eq. (15), on a square lattice $N = 16 \times 480$ (open dots). For comparison, Υ for a square lattice $N = 80 \times 80$ is also shown (stars). The inset shows the distribution function $f(i_{\rm tot})$ at $T = 0.5T_{\rm KT}$ (closed dots), $0.6T_{\rm KT}$ (open dots), and $0.7T_{\rm KT}$ (closed squares); here $T_{\rm KT} = 0.445J/k_B$.

that without randomness. In the present case, the multipeak structure in $f(i_{\rm tot})$ disappears at lower temperatures, because vortex pairs can be easily created in the presence of surface randomness. This may imply that ρ_p can be observed at lower temperatures in the presence of randomness. However, a high density of vortex pairs does not necessarily result in dissipation of superflow. If vortices are strongly pinned, they do not contribute to dissipation.

We also consider the effect of surface randomness to the helicity modulus in bars. We introduce uniform randomness $[0 < J(\boldsymbol{n},\boldsymbol{n}') < J]$ only to bonds between surface spins. Figure 13 shows the result. The helicity modulus is only slightly affected by the surface randomness; the value at $T = 0$ is reduced from unity, but the onset temperature is hardly affected both in a bar and the bulk. The multipeak structure in the distribution function disappears more rapidly than that without randomness, reflecting larger number of vortex excitations in the system.

VI. SUMMARY AND DISCUSSION

We have studied helicity modulus Υ in quasi-one-dimensional classical XY models. In quasi-one-dimension, the distinction between ρ_s, the coefficient of the increase in the free energy in the presence of infinitesimal phase gradient,

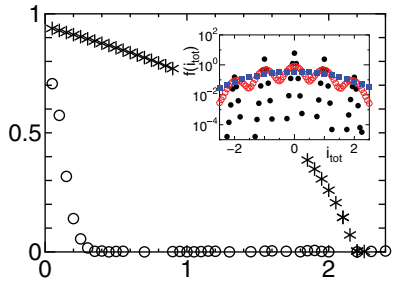

FIG. 13. (Color online) Helicity modulus Υ in the 3D XY model ($N = 4 \times 4 \times 480$) where exchange interactions between surface bonds are uniformly distributed between 0 and J. For comparison, Υ for a cubic lattice ($N = 40 \times 40 \times 40$) is also shown (stars). The inset shows the distribution function $f(i_{\rm tot})$ at $T = 0.2T_\lambda$ (closed dots), $0.3T_\lambda$ (open dots), and $0.4T_\lambda$ (closed squares); $T_\lambda = 2.20J/k_B$.

and ρ_p, the coefficient of the increase in the free energy under a twisted boundary condition, is essential. It is ρ_p that is proportional to Υ calculated under the conventional periodic boundary condition. However, which one, ρ_s or ρ_p, is observed in an experiment depends on the condition under which the experiment is carried out; for example, it depends on the value of $\omega\tau$.

We proposed two methods to calculate the helicity modulus that is proportional to ρ_s. One method is to calculate Υ with eliminating phase slippage using a specific boundary condition, the no-phase-slippage boundary condition (NPSBC). This method is readily applied to other classical and quantum lattice systems. The other is to restrict the Monte Carlo sampling to those with small phase winding, $|i_{\rm tot}| \leqslant 1/2$. Both methods have some limitations; for example, neither method can be directly applied to continuous models. However, we have found that consistent results can be obtained with the two methods. We have found that the results obtained with the two methods agree well at low temperatures, and that both methods give Υ that survives at such a high temperature as $T_{\rm KT}$ (in films) or T_λ (in bars) even in the one-dimensional limit, $L_{\rm eff} \gg 1$. At $T \gtrsim T_{\rm KT}$, $\rho_s(T)$ remains finite and it is larger for a smaller L_x in films. This implies that the confinement mechanism discussed in rather wide pores[20–22] also holds in narrower channels. With the restricted sampling method, $\rho_s(T)$ is overestimated at $T \gtrsim T_{\rm KT}$ in films and at $T \gtrsim T_\lambda$ in bars. This is because thermally excited vortices make the distribution function so broad that it is unjustifiable to restrict the sampling to $|i_{\rm tot}| \leqslant 1/2$. In this connection, we noted that the strictly one-dimensional case is different from the quasi-one-dimensional cases because no free vortices contribute the dissipation of superflow in one dimension (see Appendix C).

Next, we discussed a difference between films and bars. In films, the density of vortex pairs is so low, $\sim 4 \times 10^{-3}$, even at $T = T_{\rm KT}$, that the free-energy barrier that the system has to overcome for phase slippage to occur remains finite at temperatures close to $T_{\rm KT}$. This makes the observation of ρ_p rather difficult in a dynamical experiment such as a torsional oscillator experiment. Then, it would be possible to observe finite superfluid density ρ_s at temperatures close to $T_{\rm KT}$ in films. On the other hand, in bars, the free-energy barriers disappear at temperatures much lower than T_λ, say $T = 0.6T_\lambda$, because of proliferating thermally excited vortices. This makes the observation of ρ_p relatively easy in bars. Then, it is likely that one can observe the onset of superfluidity characteristic of quasi-one-dimension, that is, the onset at a temperature much lower than the bulk transition temperature T_λ, in bars.[50]

Now, we discuss the experiments on quasi-one-dimensional ^{4}He in the light of the results in this study. In the torsional oscillator experiments on ^{4}He filling nanopores, a second increase in the resonance frequency was observed at a temperature below $T = T_\lambda$;[9–11] however, no clear second increase was observed in ^{4}He films.[3,4] These observations are qualitatively consistent with the results obtained in this study: ρ_p is more likely to be observed in bars than in films.

Taniguchi *et al.* estimated the value of ΔE_0, which corresponds to ΔF in this study, as approximately 2 K ($\simeq T_\lambda$)[11] from the dissipation at low temperatures $T \lesssim 0.3T_\lambda$. This is a small value compared to the one obtained in this study; we found

that $\Delta F \gtrsim (7–8)J \simeq 3.5T_\lambda$. Furthermore, it was reported that in pores of diameter 24 Å, there occurs a second increase of the frequency shift at $T \simeq 0.2$ K $\simeq 0.1T_\lambda$.[51] This may also imply a smaller value of ΔF. As we discussed in Sec. V, surface randomness may help in reducing ΔF; however, it is not clear how far vortices created in the presence of surface randomness can freely drift. In addition to randomness, the effect of adsorption potential may also be important. In the presence of adsorption potential, it is natural that a He system filling pores is not uniform. For example, the density near the surface can be higher than that in the center of pores and superfluid density can be smaller near the surface than that in the central part. Adsorption potential is unfavorable at least for exchange processes in the normal direction of the surface. Then, it is possible that vortices are more easily excited as we found in the case of surface randomness, where the exchange interactions on the surface were also weakened. Quantitative comparison requires a precise knowledge of adsorption potential of the substrate; it is beyond the scope of this study.

In the experiment on He films in nanopores of diameter 24 Å, a second gradual increase in the resonance frequency was also reported.[12] However, no clear second increase has been observed in pores of other values of diameter. It is possible that surface randomness plays a role, and further investigation is necessary to reach a reliable conclusion.

To understand the experiments on quasi-one-dimensional He more accurately, it may be necessary to perform calculations that take account of precise microscopic details of the system such as adsorption potential. The methods to calculate ρ_s proposed in this study are not directly applicable to continuous models. It is desirable to develop a universal method to calculate ρ_s. Another possibility is to simulate the real-time evolution of the system directly.[52,53] These problems are important subjects of future studies.

ACKNOWLEDGMENTS

We thank N. Wada, M. Hieda, and T. Matsushita for useful discussions and comments. One of the authors (Y.K.) is supported by Japan Society of Promotion of Science. This work was completed while one of the authors (D.S.H.) stayed at Royal Holloway, University of London. D.S.H. is grateful to J. Saunders for kind hospitality. We thank S. Pandey for critically reading the manuscript.

APPENDIX A: HELICITY MODULUS IN A BAR WITH AN OCTAGONAL CROSS SECTION

In contrast to a film, a bar (with square sections) has corners. Corner spins have 4 nearest neighbors in contrast to the other surface spins, which have 5 nearest neighbors. This means that vortices tend to be created near corners, because the energy cost can be smaller. To study the effect of corners, we consider bars with a different cross section, an octagonal cross section, where all the surface spins have 5 nearest neighbors. See the inset of Fig. 14.

Figure 14 shows the temperature dependence of Υ of a bar ($N = 12 \times 480$). Here, we plot Υ as a function of $L_{\rm eff}T$. For the bar studied here, $L_{\rm eff} = 480/12 = 40$. This result agrees with that for a bar with corners ($N = 4 \times 4 \times 480$). Thus, the helicity modulus is little affected by the shape of the cross section.

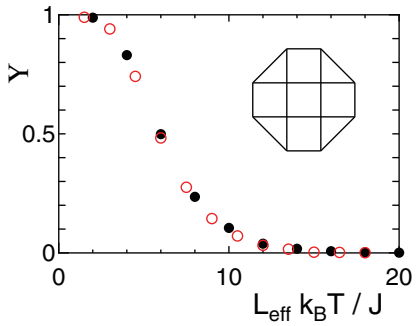

FIG. 14. (Color online) Temperature dependence of helicity modulus Υ in a bar of size $N = 12 \times 480$ (open dots), whose cross-section view is shown in the inset; $L_{\rm eff} = 480/12 = 40$. For comparison, the result for $N = 4 \times 4 \times 480$ is also shown (closed dots).

The energy necessary for vortex creation is larger than that in a bar with a square cross section. For a bar of size $N = 4 \times 4 \times 480$, we found $E_v/J = 7.75 \pm 0.02$, and in the present case, we find that $E_v/J = 9.13 \pm 0.01$; this is larger than the value for $N = 40 \times 40 \times 40$. As can be seen in Fig. 15, at $T = 0.4T_\lambda$, the multipeak structure is more prominent than that in the case of a bar with a square cross section [Fig. 7(b)]. However, the multipeak structure is completely washed out at $T = 0.6T_\lambda$, as in Fig. 7(b). Therefore, the conclusion that the free-energy barrier ΔF decreases more rapidly in bars than that in films is valid irrespective of the details of the shape of the cross section of a bar.

APPENDIX B: BULK CASES

We summarize the results in the bulk cases, that is, the results on a lattice measuring $L \times L(\times L)$. Figure 16 compares the helicity modulus Υ calculated with different boundary conditions or methods, that is, the conventional boundary condition, the NPSBC, and the RS. It can be seen that the results agree well with each other. This is because, in the bulk cases, the contribution of phase slippage to superfluid density is negligible from the beginning. We obtain similar results whether the effect of phase slippage is suppressed or not. However, by close inspection, we note that Υ calculated with the RS at $N = 160 \times 160$ does not vanish and stays

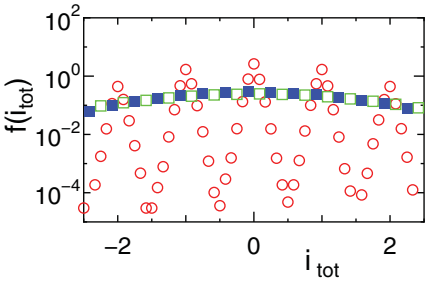

FIG. 15. (Color online) Distribution function $f(I_{\rm tot})$ of phase winding $i_{\rm tot}$ for a bar of size $N = 12 \times 480$ at different temperatures: $0.4T_\lambda$ (open dots), $0.6T_\lambda$ (closed squares), and T_λ (open squares).

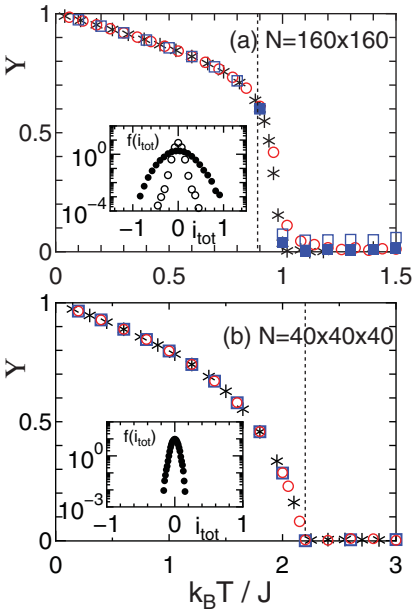

FIG. 16. (Color online) (a) Helicity modulus Υ in a film of size $N = 160 \times 160$ calculated with the conventional boundary condition (stars), the NPSBC (dots), and the RS (open squares). Closed squares represent results obtained with the RS where the restriction of $|i_{\rm tot}| \leqslant 0.7$ is imposed on the sampling. The inset shows the distribution function $f(i_{\rm tot})$ of phase winding calculated with the conventional boundary condition at $T = T_{\rm KT}$ (open dots) and $1.5T_{\rm KT}$ (closed dots). The vertical dotted line stands for the KT transition temperature $T_{\rm KT} = 0.89J/k_B$. (b) Helicity modulus Υ in a bar of size $N = 40 \times 40 \times 40$ calculated with the conventional boundary condition (stars), the NPSBC (dots), and RS (squares). The inset shows the distribution function $f(i_{\rm tot})$ of phase winding calculated with the conventional boundary condition at $T = 1.5T_{\rm KT}$. The vertical dotted line stands for the bulk transition temperature $T_\lambda = 2.20J/k_B$.

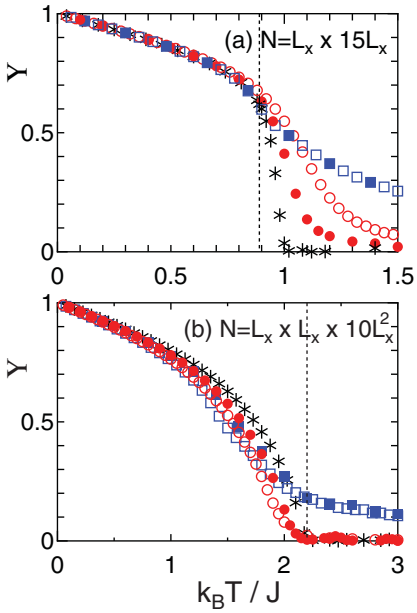

FIG. 17. (Color online) (a) Helicity modulus Υ in a film of effective length $L_{\rm eff} = L_z/L_x = 15$, calculated with the NPSBC [$L_x = 16$ (open dots) and 48 (closed dots)] and the RS [$L_x = 16$ (open squares) and 32 (closed squares)]. For comparison, Υ in a film of size $N = 160 \times 160$ calculated with the conventional boundary condition is shown with stars. The vertical dotted line stands for the KT transition temperature $T_{\rm KT} = 0.89J/k_B$. (b) Helicity modulus Υ in a bar of effective length $L_{\rm eff} = L_z/L_x^2 = 10$, calculated with the NPSBC [$L_x = 6$ (open dots) and 10 (closed dots)] and the RS [$L_x = 6$ (open squares) and 10 (closed squares)]. For comparison, Υ in a bar of size $N = 40 \times 40 \times 40$ calculated with the conventional boundary condition is shown with stars. The vertical dotted line stands for the bulk transition temperature $T_\lambda = 2.20J/k_B$.

constant ($\sim$0.06) at $T > T_{\rm KT}$. This is because the distribution function $f(i_{\rm tot})$ fairly spreads and the effect of vortices is not completely taken into account with the RS at $T > T_{\rm KT}$. In the inset of Fig. 16(a), we show the distribution function $f(i_{\rm tot})$ of phase winding calculated with the conventional boundary condition (used in Sec. II) at $T = T_{\rm KT}$ and $1.5T_{\rm KT}$. At $T = T_{\rm KT}$, $f(i_{\rm tot})$ is localized around $i_{\rm tot} = 0$ so well that the contributions of vortices are fully considered with the restriction of $|i_{\rm tot}| \leqslant 1/2$. However, at $T = 1.5T_{\rm KT}$, $f(i_{\rm tot})$ is spread so widely that the restriction $|i_{\rm tot}| \leqslant 1/2$ is too strong to consider the contributions of vortices accurately. If we relax the restriction, Υ readily vanishes at $T > T_{\rm KT}$. Indeed, we find that Υ vanishes within statistical errors at $T > T_{\rm KT}$ with the restriction $|i_{\rm tot}| \leqslant 1$. When temperature further increases from $T = 1.5T_{\rm KT}$, we find no further significant spreading of $f(i_{\rm tot})$. One may expect that additional peaks appear around $i_{\rm tot} = \pm 1$ at $T \gg J/k_B$, but we find only a weak change in the slope of $f(i_{\rm tot})$ around $i_{\rm tot} = \pm 1$ at $T \gg J/k_B$. In bars ($N = L \times L \times L$), the distribution function is well localized around $i_{\rm tot} = 0$ [see the inset of Fig. 16(b)], and the RS gives results in good agreement with those obtained with the conventional boundary condition even at higher temperatures. Here, the energy of a state with a finite $i_{\rm tot}$ is of the order $O(L)$; the contribution from such a state is negligible at any temperature when $L \to \infty$.

Next, we briefly discuss the approach to the bulk results obtained with the conventional boundary condition. Figure 17(a) shows Υ in films of effective length $L_{\rm eff} = L_z/L_x = 15$ calculated with the NPSBC and RS. It can be seen that the bulk limit is approached with the NPSBC as the system size increases

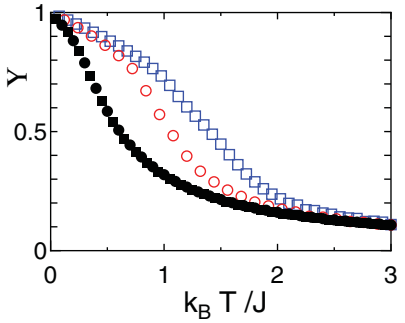

FIG. 18. (Color online) Helicity modulus Υ of the one-dimensional XY model with different sizes calculated with the restricted sampling (RS) : $L_z = 100$ (closed dots) and 200 (closed squares). For comparison, Υ's in a film $N = 16 \times 480$ (open dots) and in a bar $N = 4 \times 4 \times 480$ (open squares) calculated with the RS are also shown.

at any temperature although at a slower rate at $T > T_{\rm KT}$. On the other hand, the results obtained with the RS are weakly size dependent, and the bulk limit is not reached at $T > T_{\rm KT}$. In the quasi-one-dimensional case, that is, $L_{\rm eff} = L_z/L_x \gg 1$, the distribution function $f(i_{\rm tot})$ is broadened significantly at $T_{\rm KT}$ even when $L_x, L_z \gg 1$, and the effects of vortices are only partly considered with the RS. Figure 17(b) shows Υ in bars of effective length $L_{\rm eff} = L_z/(L_x L_y) = 10$ calculated with the NPSBC and RS. Similarly to the case with films, the bulk limit is obtained only with the NPSBC. The helicity modulus calculated with the RS decreases only gradually as temperature increases. In Appendix C, we compare results obtained using the RS in films and bars with those obtained in purely one-dimensional systems. Instead of using a fixed value of $L_{\rm eff}$, we can increase the system size with a fixed value of $L_z/L_x = L_z/L_y$. In this case, the effective length $L_{\rm eff}$ decreases as the system size increases and the bulk limit is naturally obtained even with the RS.

APPENDIX C: HELICITY MODULUS IN ONE DIMENSION

We can also calculate the helicity modulus in one-dimensional classical XY models. In one dimension, the direct application of the no-phase-slippage boundary condition makes no sense and we calculate helicity modulus with the restricted sampling (RS). In one dimension, $I_{\rm tot}(=i_{\rm tot})$ assumes only integer values. Then, the RS implies that we calculate Υ using those samples with $I_{\rm tot} = 0$. Figure 18 shows the results for the one-dimensional XY model with $L_z = 100$ and 200. The restriction $I_{\rm tot} = 0$ implies the strict imposition of momentum conservation. That is why Υ remains finite at high temperatures. The results for films and bars converge to the result in one dimension at high temperatures when the RS is used. This also shows that the helicity modulus calculated with the RS overestimates ρ_s. In films and bars, thermally excited vortices significantly contribute to dissipation of superflow and diminish helicity modulus at high temperatures. In the RS, the effect is fully considered at low temperatures where the central peak in the distribution function $f(i_{\rm tot})$ is well localized. However, as T increases, the width of the central peak increases rapidly and can far exceed unity at high temperatures. In those cases, using the restrictions $|i_{\rm tot}| \leqslant 1/2$, we consider only a limited portion of the contributions from vortices. The results then converge to that in purely one dimension.

[1] N. Wada, J. Taniguchi, H. Ikegami, S. Inagaki, and Y. Fukushima, Phys. Rev. Lett. **86**, 4322 (2001).

[2] J. Taniguchi, A. Yamaguchi, H. Ishimoto, H. Ikegami, T. Matsushita, N. Wada, S. M. Gatica, M. W. Cole, F. Ancilotto, S. Inagaki, and Y. Fukushima, Phys. Rev. Lett. **94**, 065301 (2005).

[3] H. Ikegami, Y. Yamato, T. Okuno, J. Taniguchi, N. Wada, S. Inagaki, and Y. Fukushima, Phys. Rev. B **76**, 144503 (2007).

[4] R. Toda, M. Hieda, T. Matsushita, N. Wada, J. Taniguchi, H. Ikegami, S. Inagaki, and Y. Fukushima, Phys. Rev. Lett. **99**, 255301 (2007).

[5] V. L. Berezinskii, Sov. Phys. JETP **34**, 610 (1972).

[6] J. M. Kosterlitz and D. J. Thouless, J. Phys. C **6**, 1181 (1973).

[7] J. M. Kosterlitz, J. Phys. C **7**, 1046 (1974).

[8] D. R. Nelson and J. M. Kosterlitz, Phys. Rev. Lett. **39**, 1201 (1977).

[9] J. Taniguchi and M. Suzuki, J. Low Temp. Phys. **150**, 347 (2008).

[10] J. Taniguchi, R. Fujii, and M. Suzuki, J. Phys. Conf. Ser. **150**, 032108 (2009).

[11] J. Taniguchi, Y. Aoki, and M. Suzuki, Phys. Rev. B **82**, 104509 (2010).

[12] N. Wada, Y. Minato, T. Matsushita, and M. Hieda, J. Low Temp. Phys. **162**, 549 (2011).

[13] J. E. Berthold, D. J. Bishop, and J. D. Reppy, Phys. Rev. Lett. **39**, 348 (1977).

[14] B. C. Crooker, B. Hebral, E. N. Smith, Y. Takano, and J. D. Reppy, Phys. Rev. Lett. **51**, 666 (1983).

[15] E. D. Adams, K. Uhlig, Y.-H. Tang, and G. E. Haas, Phys. Rev. Lett. **52**, 2249 (1984).

[16] J. R. Beamish, A. Hikata, L. Tell, and C. Elbaum, Phys. Rev. Lett. **50**, 425 (1983).

[17] Cao Lie-zhao, D. F. Brewer, C. Girit, E. N. Smith, and J. D. Reppy, Phys. Rev. B **33**, 106 (1986).

[18] K. Yamamoto, H. Nakashima, Y. Shibayama, and K. Shirahama, Phys. Rev. Lett. **93**, 075302 (2004).

[19] S. I. Shevchenko, Sov. J. Low Temp. Phys. **14**, 553 (1988).

[20] J. Machta and R. A. Guyer, Phys. Rev. Lett. **60**, 2054 (1988).

[21] T. Minoguchi and Y. Nagaoka, Prog. Theor. Phys. **80**, 397 (1988).

[22] J. Machta and R. A. Guyer, J. Low Temp. Phys. **74**, 231 (1989).

[23] In Ref. 22, they used σ_p for the present ρ_p. In Ref. 25, $\rho_s^{(F)} = \rho_p$, and in Ref. 29, $\rho_s^{\rm HM} = \rho_p$.

[24] It should also be noted that the superfluid velocity v_t caused by a torsional oscillator is usually much smaller than the velocity v_q of quantized superflow. Typically, $v_t \simeq 10^{-4}$ cm/s whereas $v_q \simeq 2\pi\hbar/(m\ell_z) \simeq 30$ cm/s for $\ell_z \simeq 3000$ Å.[29]

[25] N. V. Prokof'ev and B. V. Svistunov, Phys. Rev. B **61**, 11282 (2000).

[26] R. G. Melko, A. W. Sandvik, and D. J. Scalapino, Phys. Rev. B **69**, 014509 (2004).

[27] N. V. Prokof'ev, B. V. Svistunov, and I. S. Tupitsyn, JETP **87**, 310 (1998).

[28] M. Boninsegni, A. B. Kuklov, L. Pollet, N. V. Prokof'ev, B. V. Svistunov, and M. Troyer, Phys. Rev. Lett. **99**, 035301 (2007).

[29] K. Yamashita and D. S. Hirashima, Phys. Rev. B **79**, 014501 (2009); J. Low Temp. Phys. **162**, 617 (2011).

[30] A. Del Maestro and I. Affleck, Phys. Rev. B **82**, 060515(R) (2010).

[31] M. Tsukamoto and M. Tsubota, J. Low Temp. Phys. **162**, 603 (2011).

[32] T. Matsubara and H. Matsuda, Prog. Theor. Phys. **16**, 569 (1956).

[33] A. Görlitz, J. M. Vogels, A. E. Leanhardt, C. Raman, T. L. Gustavson, J. R. Abo-Shaeer, A. P. Chikkatur, S. Gupta, S. Inouye, T. Rosenband, and W. Ketterle, Phys. Rev. Lett. **87**, 130402 (2001).

[34] F. Schreck, L. Khaykovich, K. L. Corwin, G. Ferrari, T. Bourdel, J. Cubizolles, and C. Salomon, Phys. Rev. Lett. **87**, 080403 (2001).

[35] B. Paredes, A. Widera1, V. Murg, O. Mandel, S. Fölling, I. Cirac, G. V. Shlyapnikov, T. W. Hänsch, and I. Bloch, Nature (London) **429**, 277 (2004).

[36] T. Kinoshita, T. Wenger, and D. S. Weiss, Science **305**, 1125 (2004).

[37] U. Wolff, Phys. Rev. Lett. **62**, 361 (1989).

[38]S. Teitel and C. Jayaprakash, Phys. Rev. B **27**, 598 (1983).
[39]M. E. Fisher, M. N. Barber, and D. Jasnow, Phys. Rev. A **8**, 1111 (1973).
[40]J. Tobochnik and G. V. Chester, Phys. Rev. B **20**, 3761 (1979).
[41]In a narrow bar, say $N = 4 \times 4 \times 480$, vortex rings are hardly observed in Monte Carlo snapshots; vortices easily "touch" the surface. As a bar gets wider, the number of vortex rings increases.
[42]M. Hasenbusch, J. Phys. A **38**, 5869 (2005), and references therein.
[43]In contrast to Eq. (2), this expression is given in terms of J, not $\rho_s(T)$. That is why a simple closed-form expression such as Eq. (2) is not obtained.
[44]A. P. Gottlob and M. Hasenbusch, Physica A (Amsterdam) **201**, 593 (1993), and references therein.
[45]C. Bowen, D. L. Hunter, and N. Jan, J. Stat. Phys. **69**, 1097 (1992).
[46]R. Gupta and C. F. Baillie, Phys. Rev. B **45**, 2883 (1992).
[47]For $N = 4 \times 4 \times 480$, the corresponding temperature range is $0.50J \lesssim k_B T \lesssim 0.72J$. For a wider bar, the temperature range shifts to higher temperatures. For $N = 40 \times 40 \times 40$, $0.58J \lesssim k_B T \lesssim 0.81J$.
[48]In 1D, the temperature dependence of the relaxation time is shown to follow the power law. See, for example, Yu. Kagan, N. V. Prokof'ev, and B. V. Svistunov, Phys. Rev. A **61**, 045601 (2000). However, it is not obvious whether the theory is applicable to He in nanopores, which is not strictly one dimensional.
[49]To impose the NPSBC in a bar, we can choose any one of the $L_x \times L_y$ rows and replace the spin in the row with a single spin.
[50]This does not necessarily mean that $\rho_p(T)$ is observed in the whole temperature range below $T = T_\lambda$. If $\omega\tau \gg 1$ at $T = 0$ and $\omega\tau \ll 1$ at $T \gtrsim T_o(<T_\lambda)$, the observed superfluid density crossovers from $\rho_s(T)$ (at $T \ll T_o$) to $\rho_p(T)$ at $T \simeq T_o$. If T_o is higher than the onset temperature of $\rho_p(T)$, which is suggested in the present study, the observed onset temperature is T_o.
[51]In this experiment, pores are filled with He, but the samples are not immersed in bulk He. The outer surface is covered with He film and the KT transition was observed. This condition, different from the other experiments,[3,4,10,11] may have a peculiar effect on superfluid density.
[52]G. Vidal, Phys. Rev. Lett. **93**, 040502 (2004).
[53]I. Danshita and C. W. Clark, Phys. Rev. Lett. **102**, 030407 (2009).